Bioorganic & Medicinal Chemistry 18 (2010) 5123–5128

Contents lists available at ScienceDirect

Bioorganic & Medicinal Chemistry

journal homepage: www.elsevier.com/locate/bmc

STD-NMR studies of two acceptor substrates of GlfT2, a galactofuranosyltransferase from *Mycobacterium tuberculosis*: Epitope mapping studies

Monica G. Szczepina [a], Ruixiang B. Zheng [b], Gladys C. Completo [b], Todd L. Lowary [b,*], B. Mario Pinto [a,*]

[a] Department of Chemistry, Simon Fraser University, Burnaby, British Columbia, Canada V5A 1S6
[b] Department of Chemistry and Alberta Ingenuity Centre for Carbohydrate Science, Gunning-Lemieux Chemistry Centre, University of Alberta, Edmonton, Alberta, Canada T6G 2G2

ARTICLE INFO

Article history:
Received 13 March 2010
Revised 23 May 2010
Accepted 25 May 2010
Available online 4 June 2010

Keywords:
STD-NMR
Epitope mapping
Galactofuranosyltransferase
GlfT2
Trisaccharide substrates

ABSTRACT

The major structural component of the mycobacterial cell wall, the mycolyl–arabinogalactan–peptidoglycan complex, possesses a galactan core composed of approximately 30 galactofuranosyl (Gal*f*) resides attached via alternating β-(1→6) and β-(1→5) linkages. Recent studies have shown that the entire galactan is synthesized by two bifunctional galactofuranosyltransferases, GlfT1 and GlfT2. We report here saturation transfer difference (STD) NMR studies GlfT2 using two trisaccharide acceptor substrates, β-D-Gal*f*-(1→6)-β-D-Gal*f*-(1→5)-β-D-Gal*f*-O$(CH_2)_7CH_3$ (**2**) and β-D-Gal*f*-(1→5)-β-D-Gal*f*-(1→6)-β-D-Gal*f*-O$(CH_2)_7CH_3$ (**3**), as well as the donor substrate for the enzyme, UDP-Gal*f*. Epitope mapping demonstrated a greater enhancement toward the 'reducing' ends of both trisaccharides, and that UDP-galactofuranose (UDP-Gal*f*) made more intimate contacts through its nucleotide moiety. This observation is consistent with the greater flexibility required within the active site of the reaction between the growing polymer acceptor and the UDP-Gal*f* donor. The addition of UDP-Gal*f* to either **2** or **3** in the presence of GlfT2 generated a tetrasaccharide product, indicating that the enzyme was catalytically active.

1. Introduction

According to the World Health Organization, one third of the world's population is infected with *Mycobacterium tuberculosis*. Three million deaths per year are attributed to tuberculosis (TB), the most lethal bacterial infection.[1,2] The pathogenicity of the TB-causing bacterium, *M. tuberculosis*, is attributed to the mycolyl–arabinogalactan–peptidoglycan (mAGP) complex that not only encapsulates this organism but also other mycobacterial species.[3–6] Galactofuranose (Gal*f*) residues are present in a number of protozoal, fungal, and bacterial organisms,[7–9] but are absent in mammals.[10] Inhibitors of the enzymes involved in Gal*f* metabolism are therefore of interest as novel therapeutic agents.[11] The mAGP is a major structural component of the mycobacterial cell wall and serves as an essential permeability barrier, thus protecting the organism from its environment.[12]

The core of the mAGP is composed of a polymer of D-Gal*f* residues connected via alternating β-(1→5) and β-(1→6) linkages. This galactan is attached to peptidoglycan through an α-L-rhamnopyranosyl-(1→3)-2-acetamido-2-deoxy-β-D-glucopyranosyl-phosphate linkage (the linker disaccharide), and also bears three mycolylated arabinan domains (**1**, Fig. 1).[5,13] Investigation of the biosynthesis of the mAGP has identified many of the enzymes involved in this process.[12,14] The galactan domain is constructed by only two enzymes,

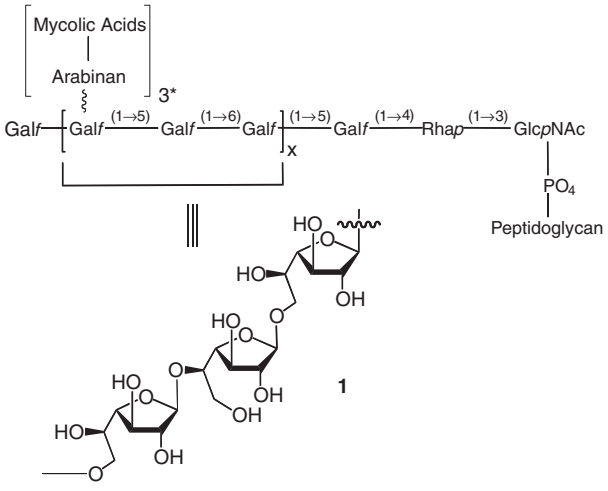

Figure 1. Structure of the mAGP complex, with the galactan region highlighted; x ~10. *The three arabinan chains have been proposed to be linked via the 8th, 10th, and 12th Gal*f* residues of the galactan core.[6]

* Corresponding authors. Tel.: +1 780 492 1861; fax: +1 780 492 7705 (T.L.L); tel.: +1 778 782 4152; fax: +1 778 782 4860 (B.M.P.).
E-mail address: bpinto@sfu.ca (B.M. Pinto).

0968-0896/$ - see front matter © 2010 Elsevier Ltd. All rights reserved.
doi:10.1016/j.bmc.2010.05.069

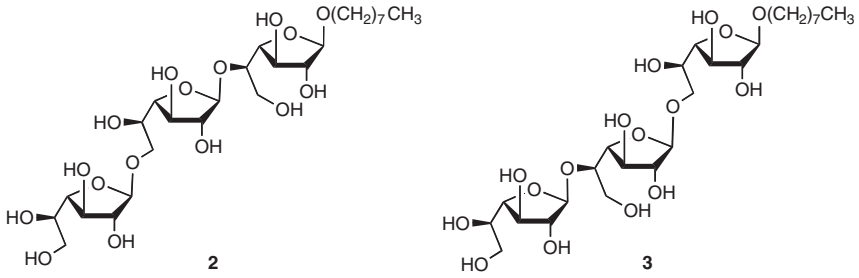

Figure 2. Trisaccharides **2** and **3**, reported acceptor substrates for GlfT2.

both of which are bifunctional.[15] One transferase, GlfT1,[16] adds the first and second Gal*f* residues to the rhamnopyranose residue in the linker disaccharide while the remaining residues are added by a second transferase, GlfT2.[17–19] Therefore, GlfT1 possesses dual Gal*f*-β-(1→4)-Rha*p*- and Gal*f*-β-(1→5)-Gal*f* transferase activity while GlfT2 affects both Gal*f*-β-(1→5)-Gal*f* and Gal*f*-β-(1→6)-Gal*f* transferase activities. As the donor species, both enzymes use UDP-galactofuranose (UDP-Gal*f*), and the acceptor substrate is the nascent biopolymer.

Studies to date indicate that the β-(1→6), β-(1→5)- and β-(1→5), β-(1→6)-linked trisaccharides **2** and **3**, respectively (Fig. 2), are efficiently galactosylated by GlfT2.[20] The former is initially a substrate for the β-(1→5)-transferase activity of the enzyme while the latter is a substrate for the β-(1→6)-transferase activity. Because the tetrasaccharide products formed from **2** and **3** are also substrates for the enzyme, subsequent additions of Gal*f* via the UDP-Gal*f* donor[20] lead to a homologous series of products. In the organism, the entire galactan structure is assembled on a polyprenol carrier before it is arabinosylated, mycolylated and finally transferred to peptidoglycan. A recent paper by Kiessling and co-workers has proposed that the ability of GlfT2 to efficiently elongate the galactan depends upon the identity of the lipid carrier.[21]

We have recently explored the bifunctionality of GlfT2,[22] in particular, we determined that one active site appears to be responsible for the assembly of β-(1→5)- and β-(1→6)-Gal*f* linkages. In order to gain further insight into the process by which GlfT2 polymerizes the galactan core of the mAG complex, we report here the use of saturation transfer difference (STD) NMR experiments with acceptor substrates **2** and **3** (Fig. 2) to obtain their epitope maps, that is, the nature of the contacts within the enzyme active site. No crystal structures of the enzyme, either unliganded or in complex with a substrate or substrate analogue, have been reported to date.

2. Experimental

2.1. Materials

Trisaccharides **2** and **3** were synthesized as described elsewhere.[23]

2.2. Preparation of GlfT2 for NMR

Expression and purification of GlfT2 has been previously described.[20] Fractions from a Sephacryl S-100 HR column were evaluated by both SDS–PAGE and a radiochemical activity assay[18] (typical specific activities were 4–6 U/mg). Fractions that were both 90% pure and active were pooled. The concentration (mg/mL) of pooled fractions was determined by UV absorption spectroscopy (A_{280} divided by 1.6, the extinction coefficient). GlfT2 (2 mg) was concentrated to ~0.5 mL using an Amicon Ultra-15 centrifuge tube with a molecular weight cut off of 30,000 Da (Millipore, Billerica, MA). To this solution was added 5 mL of phosphate buffered saline solution (50 mm Na_2HPO_4–NaH_2PO_4, 0.1 m NaCl, 10 mm $MgCl_2$, 99% D_2O; the pH of the starting buffer was 7.6) and the solution was concentrated as described above to ~0.5 mL. This procedure was then repeated five times after which the concentration, activity and purity were then again confirmed as outlined above.

2.3. NMR spectroscopy

To a sample of GlfT2 (1.6 mg) in phosphate buffered saline solution (50 mM Na_2HPO_4–NaH_2PO_4, 0.1 M NaCl, 10 mM $MgCl_2$, and 99% D_2O (pH 7.6)) was added either β-(1→6), β-(1→5) trisaccharide **2** (1.3 mg) or β-(1→5), β-(1→6) trisaccharide **3** (1.2 mg). Like many glycosyltransferases, GlfT2 is a metal-dependent enzyme and manganese Mn^{+2} is likely the natural metal ion. The metal stabilizes the binding of the sugar nucleotide donor to the protein. The enzyme is equally efficient with Mg^{+2} and that is the metal ion we have used in all our assays. The final ligand concentration was 4 mM at a ligand–protein ratio of 100:1. STD-NMR spectra with UDP-Gal*f* were acquired with 0.5 mg of UDP-Gal*f* and 1.2 mg GlfT2. Incubation of GlfT2 (1.25 mg) with UDP-Gal*f* (1.0 mg) and **2** (1.0 mg) generated the β-(1→5), β-(1→6), β-(1→5) tetrasaccharide product. The enzyme was recycled using Centricon preparation and incubated with UDP-Gal*f* (1.0 mg) and **3** (1.0 mg) to generate the β-(1→6), β-(1→5), β-(1→6) tetrasaccharide product. Ligand resonances were assigned using ^{1}H–^{1}H COSY, ^{1}H–^{1}H TOCSY, and ^{1}H–1H NOESY NMR spectroscopy. Linkages between Gal*f* residues were assigned on the basis of ^{1}H–^{1}H NOESY NMR spectra. Thus, interglycosidic NOEs were observed between H-1A and OCH_2, H-1C and H-6B as well as between H-1B and H-5A, confirming the Gal*f* ring connectivities. Water suppression using presaturation was utilized in experiments with ligand only. ^{31}P NMR spectra (at 162 MHz) were recorded on a Bruker AMX-400 NMR spectrometer. STD-NMR spectra were performed on a Bruker AMX-600 NMR spectrometer at 285 K (to slow hydrolysis) in the case of UDP-Gal*f*. STD-NMR spectra were performed on a Bruker Avance 600 NMR spectrometer, equipped with a TCI cryoprobe at 298 K in the case of the trisaccharides **2** and **3**.

Spectra were recorded with 1024 or 2048 scans and selective saturation of protein resonances at 10 ppm (30 ppm for off-resonance spectra) using a series of 40 Gaussian-shaped pulses (50 ms, 1 ms delay between pulses, $\gamma B_1/2\pi$ = 110 Hz), for a total saturation time of 2.04 s.[24] The protein resonances were broad and had significant intensity in the region downfield from 10 ppm. Irradiation at 10 ppm will result in saturation of aromatic protein resonances and via rapid spin diffusion; this saturation will also spread to aliphatic protein resonances. Irradiation at 10 ppm was also considered prudent in achieving selective saturation of the protein resonances since a ligand resonance was present at 0.8 ppm. Subtraction of saturated spectra from reference spectra was performed by phase cycling, on a Bruker AMX-600 NMR spectrometer.

Measurement of enhancement intensities was performed by direct comparison of STD-NMR spectra and reference one-dimensional ^{1}H NMR spectra. In the case of STD-NMR spectra acquired on the Bruker Avance 600 NMR spectrometer, the saturated and reference spectra were acquired simultaneously by creating a pseudo-2D experiment. The STD spectrum was obtained by subtraction of saturated spectra from reference spectra after identical processing and phasing. In all cases, the fractional STD effect was calculated by $(I_0 - I_{sat})/I_0$, where $(I_0 - I_{sat})$ is the peak intensity in the STD spectrum and I_0 is the peak intensity of an unsaturated reference spectrum. 1D-STD-NMR spectra of **2** and **3** were deconvoluted to obtain peak intensities. Carefully phased and baseline-corrected spectra were deconvoluted using a program written by Brouwer.[25] On- and off-resonance STD spectra were fit using mixed Lorentzian–Gaussian peaks with peak positions and widths held constant, and only peak intensity varied (see, e.g., Fig. S6). In all cases, STD spectra were acquired without water suppression.

STD-2D-TOCSY spectra were recorded with 16 or 32 scans per t_1 increment. A total of 256 t_1 increments were collected in an interlaced mode for the on- and off-resonance spectra. An MLEV-17 spin-lock sequence with a 10 kHz rf field strength and a mixing time of 80 ms was utilized. Rows were extracted from the STD-2D-TOCSY spectra and from the 2D-TOCSY spectra corresponding to spin systems from rings A, B, and C of trisaccharides **2** and **3** in the presence of GlfT2. Intensities ($I_{STD\text{-}2D\text{-}TOCSY}$) from the rows of the STD-2D-TOCSY spectra were referenced to the intensities ($I_{2D\text{-}TOCSY}$) from the rows of the 2D-TOCSY spectra and normalized to the selectively excited resonance. All enhancements were measured in triplicate, and the average values are shown. The error is estimated at ±10%.

Longitudinal relaxation times $T1$s of **2** and **3** in the presence of GlfT2 were determined with the inversion recovery pulse sequence.

Data processing was performed using XWINNMR (Bruker), TopSpin (Bruker), and MestReC.

3. Results

3.1. Epitope mapping of donor substrate UDP-Gal*f*

The binding of uridine 5′-diphosphate α-D-galactofuranose (UDP-Gal*f*) to GlfT2 was investigated by the use of one-dimensional STD-NMR experiments (Fig. 3). The line broadening observed is caused by ligand resonances being in close contact with the protein; the slow tumbling rate of the protein–ligand complex increases the rate of relaxation, as indicated in our previous work.[26] All of the protons of UDP-Gal*f* show some degree of enhancement, demonstrating that the entire molecule is bound in the active site of GlfT2. The largest amount of saturation transfer was observed for H-1r of the ribosyl (r) moiety and H-5u from the uracil (u) moiety, indicating that both the uracil and ribose units are making more intimate contacts with groups on the protein (Fig. 4).

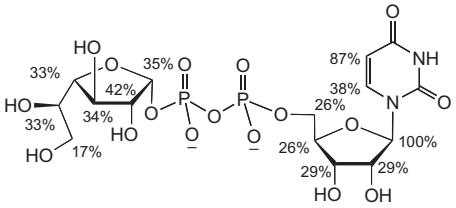

Figure 4. Epitope mapping of UDP-Gal*f* in the active site of GlfT2. Enhancements are referenced to the H-1 resonance of the ribofuranosyl moiety.

Within 5–6 h, the UDP-Gal*f* began to hydrolyze to uridine 5′-monophosphate (UMP), uridine 5′-diphosphate (UDP), Gal*f*-1-phosphate, and galactopyranose. ^{31}P NMR spectroscopy of the reaction products showed signals from UDP and UMP, as well as a signal from inorganic phosphate (from UDP hydrolysis). UDP and UMP were also observed to bind to GlfT2 (see Figs. S1, S2 in Supplementary data).

3.2. Epitope mapping of the acceptor substrate 2

The acceptor substrates **2** and **3** were examined individually for binding to GlfT2. One-dimensional STD-NMR spectra were obtained for **2** (Fig. 5). Epitope mapping revealed that the entire molecule was bound in the active site of GlfT2 and that the three Gal*f* monosaccharide units showed varying degrees of enhancement (Fig. 6).

Because only one type of monosaccharide residue (D-Gal*f*) is present in these oligosaccharides, spectral overlap was significant and this complicated analysis. For example, the overlapping resonance at 3.96 ppm comprised the H-3B, H-3C, H-3A, and H-4B signals. We attempted to estimate the contributions for each proton from STD-2D-TOCSY NMR spectra as this afforded increased spectral dispersion (see, e.g., Fig. S7).

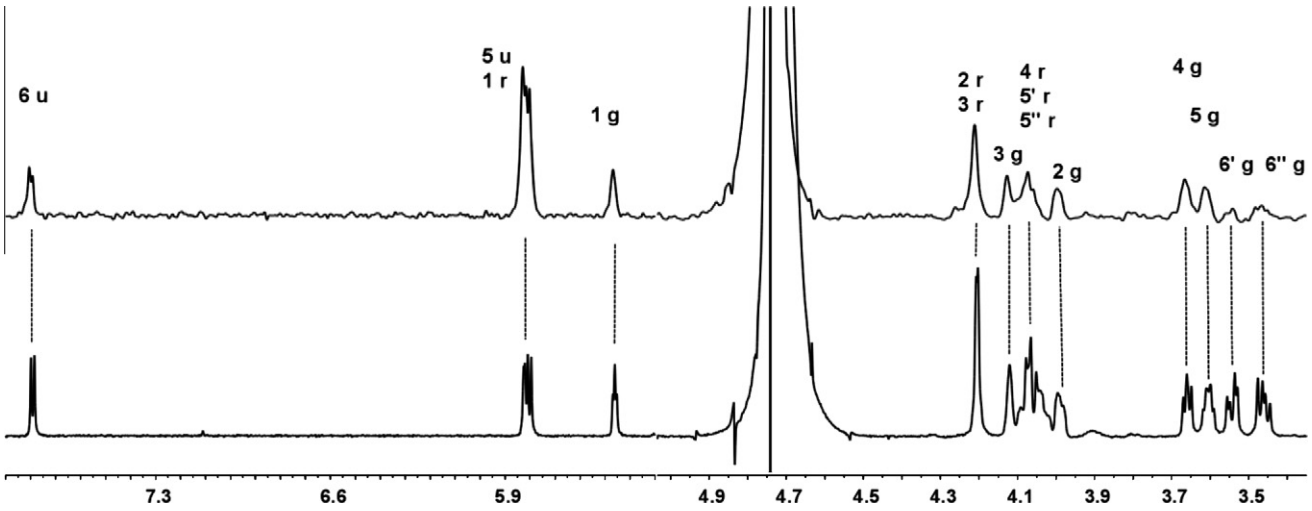

Figure 3. Expansion of 1D ^{1}H NMR (lower trace) and STD-NMR (upper trace) spectra of UDP-Gal*f* in the presence of GlfT2, at 600 MHz and 285 K. Labels g, r and u refer to Gal*f*, ribose, and uracil, respectively.

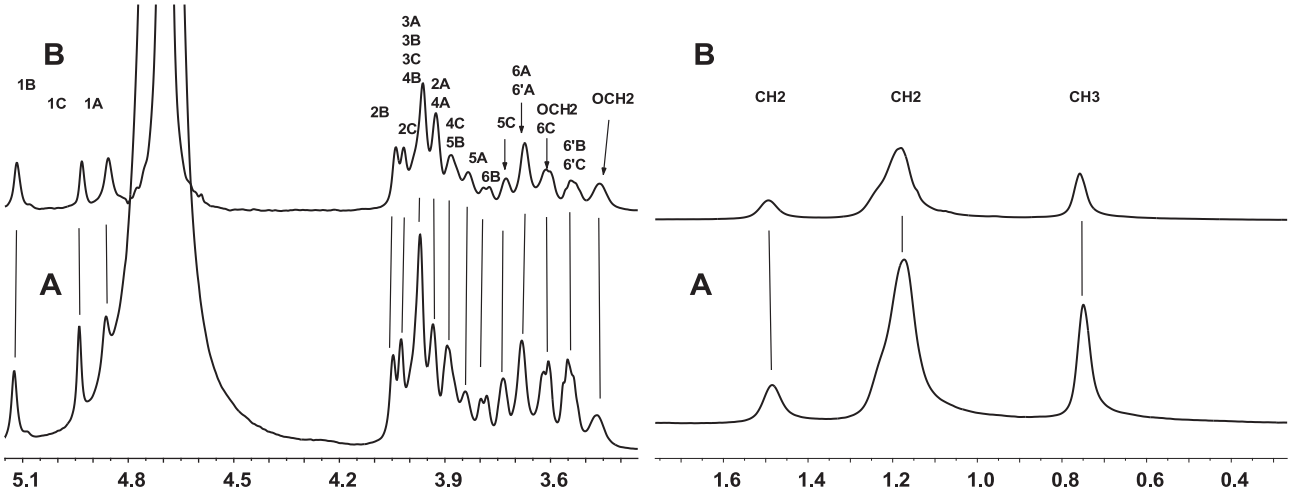

Figure 5. Expansion of (**A**) 1D ^{1}H NMR and (**B**) STD-NMR spectra of **2** at 600 MHz and 298 K in the presence of GlfT2.

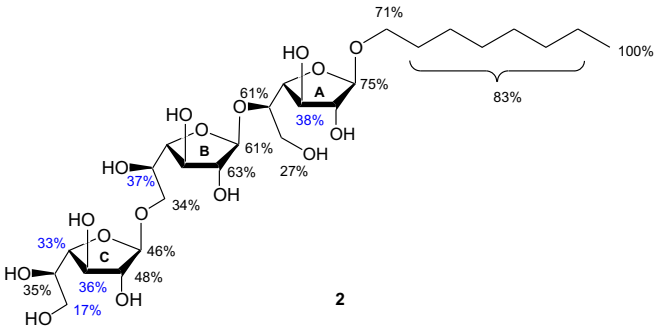

Figure 6. Epitope mapping of **2** in the active site of GlfT2. Enhancements are referenced to the methyl resonance of the octyl aglycon. Estimated enhancements from STD-2D-TOCSY NMR data are shown in blue.

Accordingly, a row was extracted from the STD-2D-TOCSY spectra corresponding to H-1A and its spin coupled partners, H-2A, H-3A, H-4A, etc. This row was referenced to the same row from the 2D-TOCSY spectra and normalized to the selectively excited resonance (H-1A in this case) indicated in bold (see Table S4). In this manner, the STD contribution from H-3A relative to H-1A could be estimated from measuring the enhancement of H-3A (52%) relative to the enhancement of H-1A (100%) in that row (see Table S4). Since the STD enhancement of H-1A is known from the 1D-STD-NMR spectrum (74.5%) (see Table S1), we can estimate the enhancement of H-3A to be 38%. We cannot assign contributions from H-2A and H-4A as these resonances are isochronous and inseparable even in the 2D spectra.

Next, we examined the contribution from H-5B as this forms part of the multiplet at 3.88 ppm (H-4C/5B). The STD contribution from H-5B relative to H-6B was estimated from a row of the STD-2D-TOCSY spectrum referenced to the same row in the 2D-TOCSY spectrum which contained H-6B and its coupled partners, H-6′B, H-5B, H-4B, etc. From this row, the enhancement of H-5B (109%) relative to the enhancement of H-6B (100%) was measured (see Table S4). Since the STD enhancement of H-6B is known from the 1D-STD-NMR spectrum (34%) (see Table S1), we can estimate the enhancement of H-5B to be 37%. We cannot assign contributions from H-3B and H-4B as these resonances are isochronous and inseparable even in the 2D spectra.

Lastly, we examined the contribution from H-3C, H-4C, and H-6C. Once again we referred to a row from both the STD-2D-TOCSY data and 2D-TOCSY data (see Table S4). Since the STD enhancement of H-5C (35%) is known from the 1D-STD-NMR spectrum (see Table S1), we can estimate the enhancements of H-3C, H-4C, and H-6C to be 36%, 33%, and 17%, respectively, from their ratios relative to H-5C in the STD-2D spectral data.

The epitope map (Fig. 6) indicates that the Gal*f* A residue makes the most intimate contacts with the protein, residue Gal*f* B makes lesser contacts, and Gal*f* C has least contacts with the protein.

An examination of the binding epitope of **2** in the presence of the donor, UDP-Gal*f* is also of interest. Thus, a sample containing UDP-Gal*f* and GlfT2 was treated with trisaccharide **2**, and the STD amplification factors for UDP-Gal*f* were calculated. The resonance from UDP-Gal*f* corresponding to H-6 uracil was not dramatically affected by the addition of trisaccharide **2**, consistent with the epitope map (Fig. 4), which indicates that it makes sparse contact with GlfT2. The STD amplification factor for the H-1r/H-5u resonance of ribose decreased by approximately 58% and that of the H-1 g resonance of galactose decreased by approximately 61%. The resonance corresponding to H-1 ribose/H-5 uracil from UDP-Gal*f* was most affected because H-1 of ribose and H-5 of uracil are critical for binding to GlfT2. During these experiments, we observed the formation of the β-(1→5), β-(1→6), β-(1→5) tetrasaccharide product, indicating that the enzyme was active and turning over (Fig. S3 in Supplementary data); however, UDP-Gal*f* hydrolysis was also observed. The STD amplification factors for **2** were not significantly affected in the presence of UDP-Gal*f*. The lack of rigidification of the acceptor deserves comment. Presumably, similar STD amplification factors were obtained because product formation is fast relative to the NMR time

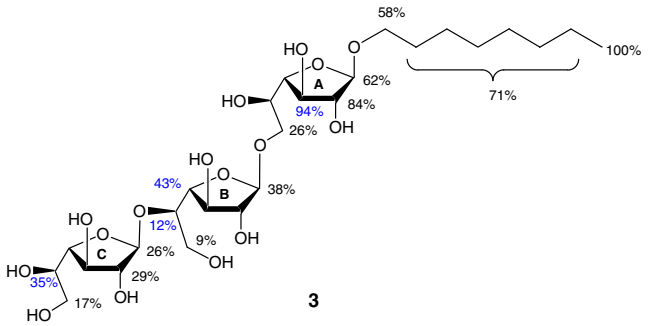

Figure 7. Epitope mapping of **3** in the active site of GlfT2. Enhancements are referenced to the methyl resonance of the octyl aglycon. Estimated enhancements from STD-2D-TOCSY NMR data are shown in blue.

scale. In addition, non-ideal substrates are being used, the natural substrates being large, membrane-associated glycolipids.

3.3. Epitope mapping of the acceptor substrate 3

Having established the manner in which GlfT2 binds **2**, the trisaccharide **3** was investigated. As with the acceptor substrate **2**, the enhancements observed in the one-dimensional STD-NMR experiments for **3** (Fig. S4 in Supplementary data) indicated that the entire molecule was bound in the active site of GlfT2. The methodology used to estimate enhancements for acceptor **2** was also used for the case of **3** (see Table S5). The epitope map for **3** is shown in Figure 7.

Taken together, these epitope mapping studies demonstrate that acceptor substrates **2** and **3** both experienced greater enhancement toward ring A, indicating that this is a critical portion of the binding epitope. These findings are consistent with a recent STD-NMR study on *N*-acetylglucosaminyl transferase V with its trisaccharide acceptor substrate.[27] In these investigations, the monosaccharide residue of the acceptor undergoing glycosylation showed lower STD effects than the other monosaccharide residues. This is presumably due to the need for this region of the substrate to be only weakly bound so that the conformational changes necessary in the glycosylation transition state can occur. Hence, it is not expected that this portion of the molecule will be tightly bound and this feature is reflected in the reduced STD enhancement.

We also examined the binding epitope of **3** in the presence of the donor, UDP-Gal*f*. As was observed with trisaccharide **2**, it was found that the addition of UDP-Gal*f* had little effect on the binding epitope of trisaccharide **3**. As seen with trisaccharide **2**, the formation of the β-(1→6), β-(1→5), β-(1→6) tetrasaccharide product was observed, indicating that the enzyme was active and turning over (Fig. S5 in Supplementary data). However, we also observed UDP-Gal*f* hydrolysis.

4. Discussion

Significant insight into the process by which the galactan portion of mycobacterial mAGP is biosynthesized has been acquired in recent years.[3–5,12,13,15] It appears that the ~30-residue long glycan is assembled by the two bifunctional galactofuranosyltransferases, GlfT1 and GlfT2.[15] Because galactan synthesis is essential for mycobacterial viability,[28] and Gal*f* appears to be absent in mammalian systems, inhibitors of these transferases could be selective therapeutic agents for the treatment of diseases such as tuberculosis and HIV-associated *Mycobacterium avium* infections.[29] It is therefore highly desirable that one gain an understanding of the structures and mechanisms of these enzymes. In this paper, we have focused on recombinant *M. tuberculosis* GlfT2.[20,30] In the absence of X-ray structural information on GlfT2 and its complexes, we used STD-NMR spectroscopy to investigate GlfT2 substrate interactions.

Epitope mapping studies with the nucleotide donor for the enzyme, UDP-Gal*f*, revealed that the strongest interactions with the protein involve the nucleotide base and H-1 of the ribose portions of the molecule. All of the hydrogens from the Gal*f* moiety also receive saturation transfer from the protein, but less than the nucleotide moiety. These trends are consistent with previous studies on the blood group B galactosyltransferase,[31] as well as *N*-acetylglucosaminyl transferase V[27] which also showed that the donor (UDP-Gal*p* and UDP-Gal*p*NAc, respectively) most strongly interacts with the protein through the nucleotide portion. This can be rationalized based on the need for the sugar that is to be transferred to be relatively loosely bound, thus facilitating molecular reorganization near the site of reaction.

Similar epitope mapping studies with two known trisaccharide substrates for the enzyme, **2** and **3**, revealed that in both cases the non-reducing end of the molecule showed lower STD effects, indicating reduced interaction with the protein. This observation is in agreement with previous studies on the binding of carbohydrate acceptor molecules by glycosyltransferases,[27,31] and, as described above for the binding of UDP-Gal*f*, is consistent with the need for the substrate to have the flexibility to participate in the enzyme-catalyzed glycosylation. If the entire acceptor and donor were tightly bound to the enzyme, it could be envisioned that the substrates would not be able to undergo the conformational distortion needed in the transition state. When these epitope mapping studies were carried out in the presence of the donor UDP-Gal*f*, the binding epitopes were not substantially different, and under these conditions the formation of a tetrasaccharide product was observed, thus demonstrating that the protein was capable of catalysis under the conditions of the experiment.

It is also of interest to note that the octyl aglycon receives substantial saturation transfer, indicating that it is interacting strongly with the protein. This is consistent with the earlier[32] observation that mycobacterial glycosyltransferases recognize oligosaccharides of long-chain alcohols better than those with shorter aglycons. In nature, GlfT2 normally recognizes, as a minimum acceptor substrate, a tetrasaccharide, the linker disaccharide plus two Gal*f* residues (see Fig. 1). Thus, the octyl group may interact with portions of the enzyme that normally bind to these additional carbohydrate residues. This proposal is consistent with the previously mentioned work from the Kiessling and co-workers, in which the nature of the aglycon of the sugar acceptor was shown to influence the outcome of GlfT2-mediated galactan elongation.[21]

In summary, these STD-NMR studies have provided additional information on substrate binding by GlfT2. When taken together with our earlier work,[22] the picture that emerges is one in which this bifunctional enzyme carries out both glycosylation reactions within a single active site, and binds its substrates in a manner similar to other glycosyltransferases.[27,31]

Acknowledgments

This work was supported by The Alberta Ingenuity Centre for Carbohydrate Science and The Natural Sciences and Engineering Research Council of Canada. We thank A. R. Lewis for performing the deconvolutions, R. Zhou for technical assistance, and D. Bleile for helpful discussions.

Supplementary data

Supplementary data (STD-NMR intensities of **2** and **3** at 298 K, and UDP-Gal*f* at 285 K, in the presence of GlfT2. *T*1 measurements of **2** and **3** at 285 K and 298 K in the presence of GlfT2. Expansion of 1D ^{1}H NMR and STD-NMR spectra of **3** at 600 MHz and 298 K in the presence of GlfT2. Expansion of 1D ^{1}H NMR and STD-NMR spectra of the hydrolysis products from UDP-Gal*f*. Expansion of 1D ^{1}H NMR spectra of **2** and UDP-Gal*f*, as well as **3** and UDP-Gal*f* in the presence of GlfT2. STD-2D-TOCSY intensities relative to 2D-TOCSY intensities of **2** in the presence of GlfT2. STD-2D-TOCSY intensities relative to 2D-TOCSY intensities of **3** in the presence of GlfT2. Deconvolution of the STD-NMR spectrum (3.2–4.2 ppm region) of **2** in the presence of GlfT2 at 298 K. STD-2D-TOCSY intensity relative to the 2D-TOCSY intensity for the selectively excited resonance H-6B of **2** in the presence of GlfT2) associated with this article can be found, in the online version, at doi:10.1016/j.bmc.2010.05.069.

References and notes

1. For perspective and current statistics: Daniel, T. M. *Respir. Med.* **2006**, *100*, 1862.
2. For perspective and current statistics: http://www.who.int/tb/en/.

3. Mahapatra, S.; Basu, J.; Brennan, P. J.; Crick, D. C. In *Tuberculosis and the Tubercle Bacillus*; Cole, S. T., Eisenach, K. D., McMurray, D. N., Jacobs, J. W. R., Eds.; American Society for Microbiology: Washington, DC, 2005; p 275.
4. Lowary, T. L. In *Glycoscience: Chemistry and Chemical Biology*; Fraser-Reid, B. O., Tatsuta, K., Thiem, J., Eds.; Springer: Berlin, 2001; Vol. 3, p 2005.
5. Besra, G. S.; Khoo, K. H.; McNeil, M. R.; Dell, A.; Morris, H. R.; Brennan, P. J. *Biochemistry* **1995**, *34*, 4257.
6. Alderwick, L. J.; Radmacher, E.; Seidel, M.; Gande, R.; Hitchen, P. G.; Morris, H. R.; Dell, A.; Sahm, H.; Eggeling, L.; Besra, G. S. *J. Biol. Chem.* **2005**, *280*, 32362.
7. de Lederkremer, R. M.; Colli, W. *Glycobiology* **1995**, *5*, 547.
8. Beverley, S. M.; Owens, K. L.; Showalter, M.; Griffith, C. L.; Doering, T. L.; Jones, V. C.; McNeil, M. R. *Eukaryot. Cell* **2005**, *4*, 1147.
9. Morelle, W.; Bernard, M.; Debeaupuis, J. P.; Buitrago, M.; Tabouret, M.; Latge, J. P. *Eukaryot. Cell* **2005**, *4*, 1308.
10. Houseknecht, J. B.; Lowary, T. L. *Curr. Opin. Chem. Biol.* **2001**, *5*, 677.
11. Richards, M. R.; Lowary, T. L. *ChemBioChem* **2009**, *10*, 1920.
12. Berg, S.; Kaur, D.; Jackson, M.; Brennan, P. J. *Glycobiology* **2007**, *17*, 35R.
13. Bhamidi, S.; Scherman, M. S.; Rithner, C. D.; Prenni, J. E.; Chatterjee, D.; Khoo, K. H.; McNeil, M. R. *J. Biol. Chem.* **2008**, *283*, 12992.
14. Tam, P. H.; Lowary, T. L. *Curr. Opin. Chem. Biol.* **2009**, *13*, 618.
15. Belanova, M.; Dianiskova, P.; Brennan, P. J.; Completo, G. C.; Rose, N. L.; Lowary, T. L.; Mikusova, K. *J. Bacteriol.* **2008**, *190*, 1141.
16. Mikusova, K.; Belanova, M.; Kordulakova, J.; Honda, K.; McNeil, M. R.; Mahapatra, S.; Crick, D. C.; Brennan, P. J. *J. Bacteriol.* **2006**, *188*, 6592.
17. Mikusova, K.; Yagi, T.; Stern, R.; McNeil, M. R.; Besra, G. S.; Crick, D. C.; Brennan, P. J. *J. Biol. Chem.* **2000**, *275*, 33890.
18. Kremer, L.; Dover, L. G.; Morehouse, C.; Hitchin, P.; Everett, M.; Morris, H. R.; Dell, A.; Brennan, P. J.; McNeil, M. R.; Flaherty, C.; Duncan, K.; Besra, G. S. *J. Biol. Chem.* **2001**, *276*, 26430.
19. Alderwick, L. J.; Dover, L. G.; Veerapen, N.; Gurcha, S. S.; Kremer, L.; Roper, D. L.; Pathak, A. K.; Reynolds, R. C.; Besra, G. S. *Protein Expr. Purif.* **2008**, *58*, 332.
20. Rose, N. L.; Completo, G. C.; Lin, S. J.; McNeil, M.; Palcic, M. M.; Lowary, T. L. *J. Am. Chem. Soc.* **2006**, *128*, 6721.
21. May, J. F.; Splain, R. A.; Brotschi, C.; Kiessling, L. L. *Proc. Natl. Acad. Sci. U.S.A.* **2009**, *106*, 11851.
22. Szczepina, M. G.; Zheng, R. B.; Completo, G. C.; Lowary, T. L.; Pinto, B. M. *ChemBioChem* **2009**, *10*, 2052.
23. Completo, G. C.; Lowary, T. L. *J. Org. Chem.* **2008**, *73*, 4513.
24. Mayer, M.; Meyer, B. *Angew. Chem., Int. Ed.* **1999**, *38*, 1784.
25. Fyfe, C. A.; Brouwer, D. H. *J. Am. Chem. Soc.* **2006**, *128*, 11860.
26. Weimar, T.; Stoffer, B.; Svensson, B.; Pinto, B. M. *Biochemistry* **2000**, *39*, 300.
27. Macnaughtan, M. A.; Kamar, M.; Alvarez-Manilla, G.; Venot, A.; Glushka, J.; Pierce, J. M.; Prestegard, J. H. *J. Mol. Biol.* **2007**, *366*, 1266.
28. Pan, F.; Jackson, M.; Ma, Y. F.; McNeil, M. *J. Bacteriol.* **2001**, *183*, 3991.
29. de Jong, B. C.; Israelski, D. M.; Corbett, E. L.; Small, P. M. *Annu. Rev. Med.* **2004**, *55*, 283.
30. Rose, N. L.; Zheng, R. B.; Pearcey, J.; Zhou, R.; Completo, G. C.; Lowary, T. L. *Carbohydr. Res.* **2008**, *343*, 2130.
31. Angulo, J.; Langpap, B.; Blume, A.; Biet, T.; Meyer, B.; Krishna, N. R.; Peters, H.; Palcic, M. M.; Peters, T. *J. Am. Chem. Soc.* **2006**, *128*, 13529.
32. Lee, R. E.; Brennan, P. J.; Besra, G. S. *Glycobiology* **1997**, *7*, 1121.